© S. Hirzel Verlag · EAA

947

The Acoustics of "A0-B0 Mode Matching" in the Violin

J. Woodhouse

Cambridge University Engineering Department, Trumpington Street, Cambridge CB2 1PZ, U.K.

Summary

It has been found by many experienced violin makers that if a violin is adjusted so as to bring two of its low-frequency modes into close proximity, then players find the result very desirable. The modes in question are a modified Helmholtz air resonance, labelled A0, and a bending mode of the whole body, neck and fingerboard, labelled B0. In this paper a simple model is developed which allows the process of "matching" these two modes to be studied. The model is shown to predict behaviour in good agreement with measurements. Implications are studied, both for instrument makers carrying out this matching, and for possible explanations of the player preference for matched instruments. It is suggested that bowing transients must play a significant role, since effects on steady tones are confined to a very few notes on the instrument.

PACS no. 43.75.De

1. Introduction

The sound and playing properties of a violin are governed by the vibration mode shapes, frequencies, damping factors and sound radiation patterns of the instrument's body. Although this statement seems obvious, it has proved remarkably difficult to uncover precise connections between the physical and perceptual behaviour, both of which are extremely complicated. An instrument maker will often ask "What will be the effect of such-and-such a constructional change?" A scientist may be able to give an answer in terms of what happens to the modes, but will generally find it much harder to say what the consequence will be for the player of the instrument, or for a distant listener. The only useful approach seems to be to nibble away at the problem by identifying particular, well-defined questions and examining them in as much depth as possible. It remains hard to answer the perceptual questions, but one may at least be able to eliminate unfruitful avenues of enquiry and pose some definite hypotheses for testing by psychoacoustical means.

In this paper, a particular empirical finding is examined in this spirit. The low-frequency modes of a violin body have been studied by a variety of experimental means. Some aspects have been understood in broad terms since the last century, other details were only revealed as new tools were developed: oscilloscopes, computer-based data acquisition and analysis systems, holographic interferometry, experimental modal analysis and so on. The state of knowledge by the early 1980s is well summarised by Cremer [1]. Since then, work to describe and classify the modes of complete violins has been particularly associated with Jansson and co-workers [2], largely based on holographic methods, and with Marshall [3], using experimental modal analysis.

The violin body consists of a number of dynamical subsystems which are coupled together. The "box" is made of thin wooden shells, plus some internal blocks to facilitate
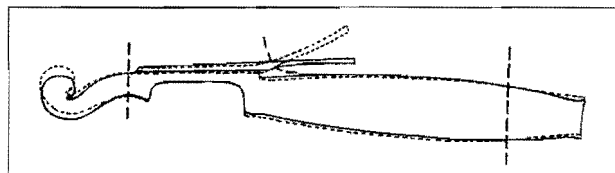
Figure 1. Cross-sectional sketch of a violin showing the body mode B0 (exaggerated, but drawn approximately to scale). Long dashed lines indicate nodes.

gluing. This structure can support coupled flexural and extensional vibration. The air space enclosed by the box, which communicates with the outside air via the f-holes, supports acoustic waves. The neck and fingerboard can support beam-like flexural and torsional vibration. The strings can support transverse vibration, of course, but also torsional and longitudinal vibration. The tailpiece, suspended between the stretched strings and the end button, can vibrate. Finally, all these subsystems are affected by the presence of the external air. This will produce added mass and damping effects from local flow, and also it allows long-range sound propagation which will provide radiation damping.

This investigation concerns two particular modes of the violin body. In their pure form, in the absence of coupling effects to be discussed below, they can be characterised as follows. One is the lowest "internal air" mode, usually labelled "A0". This has the character of a Helmholtz resonance, with air flowing in and out through the f-holes driven by variations in internal pressure which is always approximately uniform inside the box. It is significantly modified by the finite compliance of the wooden shells enclosing the box (see Cremer [1, §10.3]), so that some "breathing" motion of the back and front plates takes place. The other mode is illustrated in Figure 1. Labelled (at least by some authors) "B0", it has the character of a bending mode of the whole neck-box assembly, most of the energy being associated with cantilever-like vibration of the length of the fingerboard which projects over the front plate of the instrument. (Moral and Jansson [2] la-

bel this mode "N" rather than "B0".) For a normal violin body the mode A0 usually has a frequency in the range 275–290 Hz, while the frequency of the mode B0 can vary in the approximate range 240–340 Hz, depending particularly on the material and dimensions of the neck and fingerboard.

It has been reported by Hutchins [4], and confirmed by other instrument makers, that many players prefer instruments in which the frequencies of these two modes are very close. Players' descriptions of what is "better" about an instrument thus "matched" cover the whole gamut of "feel", sound quality and playing properties. The purpose of this article is to examine carefully the physical consequences of such "mode matching", and to attempt to focus more clearly some questions that might be asked of players in a psychoacoustical study of the phenomenon. A simple model for the acoustical and vibrational behaviour is developed and validated against experimental data. The model allows a variety of relevant transfer functions to be calculated, so that their variations during the matching process can be studied. The results also shed some light on the practical procedures which makers use when adjusting an instrument to produce matching.

2. Theory

2.1. Model equations

Several authors have discussed simple, low-dimensional models of instrument body behaviour which utilise a breakdown of the body into lumped masses and springs (e.g. Cremer [1, Chapter 10]), or by a corresponding electrical circuit (e.g. Schelleng [5], Shaw [6]). For the present purpose we can approximate the behaviour quite well with a two-degree-of-freedom model, by using the concept of generalised coordinates. The phenomenon we wish to investigate is the coupling of the pure A0 and B0 "modes" when their frequencies are close together. (If there were no coupling, it is hard to see how adjusting their relative frequencies could have much physical significance. Experimental evidence of coupling will be shown in section 3.)

Denote by $a(t)$ the amplitude of "pure A0 motion" (as would occur if the projecting fingerboard were sawn off), and correspondingly denote by $b(t)$ the amplitude of "pure B0 motion" (as would occur *in vacuo*). When small changes are made to the instrument structure to adjust the frequencies and achieve "matching", it should be a reasonable approximation to assume that no other motions of the body are involved, so that these two generalised coordinates suffice to study the behaviour. To give these amplitudes unambiguous definitions, assume that each mode shape has been mass-normalised in the usual way (see e.g. Hodges and Woodhouse [7]), so that the kinetic energy is simply

$$T = \frac{1}{2}\left[\dot{a}^2 + \dot{b}^2\right]. \tag{1}$$

The mass matrix for the system in terms of $\dot{a}, \dot{b}$ is then the unit matrix. A convention to fix the signs of a and b will be introduced in section 2.3.

The potential energy for B0 is associated with an effective structural stiffness for that mode, which we denote k. The potential energy for A0 is mainly associated with air compression inside the box. Suppose that the volume fluctuation associated with A0 motion is λa, and denote the effective stiffness of the air volume S. (In fact, this effective stiffness also includes the contribution from plate stiffness to the potential energy.) The most likely mechanism of coupling between A0-motion and B0-motion is that the B0 deformation of the body involves a small amount of volume change of the box. Suppose this volume fluctuation is $\varepsilon\lambda b$, where ε is a (presumably small) dimensionless parameter whose value will be considered later. The total potential energy of the system is now

$$V = \frac{1}{2}kb^2 + \frac{1}{2}S\left(\lambda a + \varepsilon\lambda b\right)^2, \tag{2}$$

so that the stiffness matrix is

$$K = \begin{bmatrix} \mu & \mu\varepsilon \\ \mu\varepsilon & k + \mu\varepsilon^2 \end{bmatrix} \tag{3}$$

with $\mu = S\lambda^2$.

Values of the effective stiffnesses k and μ are readily calculated as the squares of the natural (radian) frequencies of the modes B0 and A0, respectively, when the coupling ε is absent or when the frequencies are far from the "matched" state. If the frequency of A0 has the typical value 280 Hz, the required value is $\mu \approx 3.1 \cdot 10^6 \, \text{s}^{-2}$. The value of k is what has to be varied, within this model, to effect the matching. The matched state arises when, in the absence of coupling (i.e. with $\varepsilon = 0$), the two natural frequencies are equal. This happens when $k = \mu$.

2.2. Modes

From this simple model we can readily calculate the normal modes and their frequencies. The two natural frequencies ω satisfy $\det(K - \omega^2 I) = 0$, which yields

$$2\omega^2 = k + \mu\varepsilon^2 + \mu \tag{4}$$
$$\pm \sqrt{\mu^2\varepsilon^4 + 2\mu\varepsilon^2(k + \mu) + (k + \mu)^2}.$$

Notice that under "matched" conditions with $k = \mu$, and when ε is small, this reduces to

$$\omega^2 = \mu\left[1 + \frac{\varepsilon^2}{2} \pm \frac{\varepsilon}{2}\sqrt{4 + \varepsilon^2}\right] \approx \mu(1 \pm \varepsilon), \tag{5}$$

so that

$$\omega \approx \sqrt{\mu}(1 \pm \varepsilon/2). \tag{6}$$

The two natural frequencies are both displaced away from the expected value, by equal amounts above and below. This frequency separation affords an easy way to determine experimentally the value of the parameter ε. For values of k/μ different from unity, the two frequencies are always further apart: the "matched" condition gives (approximately, if terms
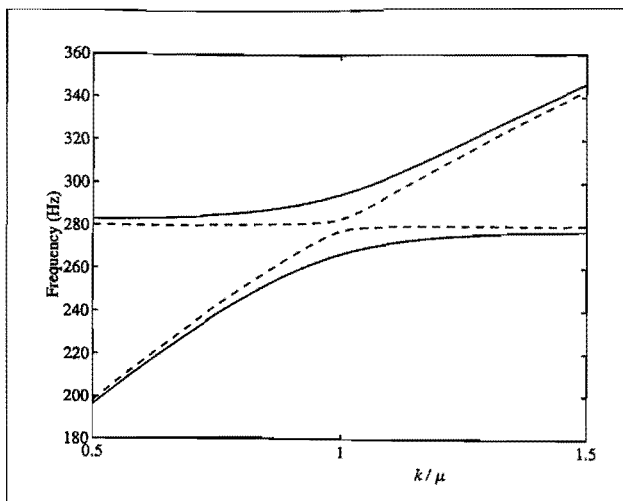
Figure 2. Behaviour of the modal frequencies given by equation (4) as k/μ is varied through the matching range, showing "veering" behaviour. Solid lines: $\varepsilon = 0.1$; dashed lines: $\varepsilon = 0.02$. The dashed lines correspond to the measured behaviour to be reported in section 4. The value $\mu \approx 3.1 \cdot 10^6$ s^{-2} is assumed, so that A0 has the typical frequency 280 Hz.

of order ε^2 are neglected) the closest approach of the two frequencies. This is illustrated in Figure 2, which shows graphs of the two solutions of (4) against k/μ for two different values of ε. The behaviour seen here is sometimes described as "veering" or "avoided crossing" (see for example Perkins and Mote [8]), for reasons which are clear from the figure. Such behaviour arises in vibrating systems of many kinds.

The mode shapes, which within this model are simply the ratios $a : b$, are given by the equation

$$K \begin{bmatrix} a \\ b \end{bmatrix} = \omega^2 \begin{bmatrix} a \\ b \end{bmatrix}, \tag{7}$$

so that

$$\frac{a}{b} = \frac{\mu\varepsilon}{\omega^2 - \mu}, \tag{8}$$

where the two different modes are found by substituting the two solutions (4) for ω^2. Notice that for the matched case and with the approximation that ε is small, this ratio reduces to the very simple result

$$\frac{a}{b} \approx \pm 1 \tag{9}$$

using (5). (The positive sign corresponds to the higher frequency if $\varepsilon > 0$, and to the lower frequency if $\varepsilon < 0$: a sign convention for a, b and ε will be introduced shortly.) This is typical curve-veering behaviour. During the matching process, as we follow one of the curves of Figure 2, the character of the modes changes continuously. The lower frequency will consist of "almost pure B0" when $k \ll \mu$, but will gradually acquire more "A0-motion" as k increases until when $k \gg \mu$ it is "almost pure A0". At the matched condition, it involves equal amplitudes of both kinds of motion, either in phase (if $\varepsilon < 0$) or in antiphase (if $\varepsilon > 0$). The higher mode follows the converse pattern.

The next stage is to estimate the damping factors of the two modes. We would expect the damping associated with B0 to be significantly lower than that associated with A0, since A0 radiates sound strongly whereas B0 does not, and the radiation damping must be added to the structural damping to obtain the total. As the character of the modes changes during the matching process, so the modal damping factors will also change. To obtain a quantitative expression we can use an argument based on Rayleigh's principle, originally used in studies of vibration damping in plates [9]. We represent the damping by allowing the two effective stiffnesses, k and μ, to become complex. Replace

$$k \rightarrow k(1 + i/Q_k), \quad \mu \rightarrow \mu(1 + i/Q_\mu), \tag{10}$$

where Q_k, Q_μ are the Q-factors of the modes B0 and A0 respectively, far from the matching condition. Now for small damping (i.e. $Q_k, Q_\mu \gg 1$) we argue that the imaginary part of the mode frequency, which will give the damping factor, can be calculated from the Rayleigh quotient using the undamped mode shapes as trial functions:

$$\Im m\{\omega^2\} \approx \frac{b^2\Im m\{k\} + (a + \varepsilon b)^2\Im m\{\mu\}}{a^2 + b^2} \tag{11}$$

using the expressions (1) and (2). Now let ω_1^2, ω_2^2 denote the two modal squared frequencies, given in the undamped case by (4). Using the expression (8) for the mode shapes, and noting that

$$\frac{1}{Q_j} \approx \frac{\Im m\{\omega_j^2\}}{\Re e\{\omega_j^2\}} \tag{12}$$

for small damping (where Q_j is the Q-factor of the jth mode), we obtain

$$\frac{1}{Q_j} \approx \frac{\dfrac{(\mu - \omega_j^2)^2 k}{Q_k} + \dfrac{\varepsilon^2\omega_j^4\mu}{Q_\mu}}{\omega_j^2\left[\mu^2\varepsilon^2 + (\mu - \omega_j^2)^2\right]}, \quad j = 1, 2, \tag{13}$$

where ω_1^2 and ω_2^2 are the values given by (4). The variation of Q_1 and Q_2 during the matching process is illustrated in Figure 3. This shows the same range of k and the same two values of ε as Figure 2. The assumed values of Q_k and Q_μ are 80 and 25 respectively.

2.3. Transfer functions

The final stage of modelling is to calculate some relevant transfer functions, which show the overall effect of the matching process, and which can be compared with measurements in order to validate the model and determine the parameter values. For normal playing, the input to the body is provided by transverse vibration in the bowing plane of one of the strings. Any corresponding transfer function will have as input a force $F e^{i\omega t}$ applied at the string notch in the bridge, in the plane of bowing. For definiteness we will consider excitation at the G-string notch, which is convenient for comparison with measurements.
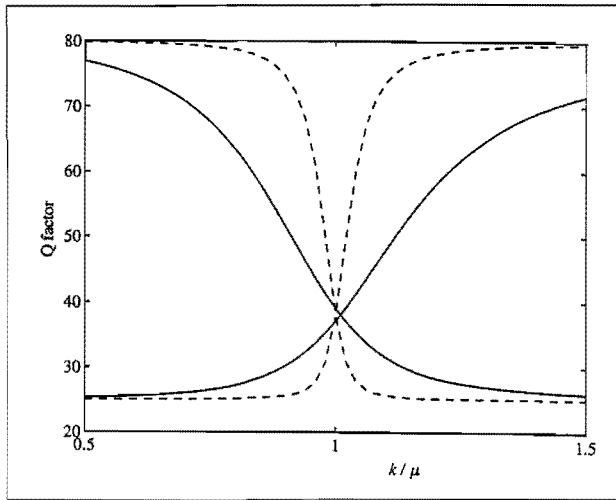
Figure 3. Variation of modal Q factors as k/μ is varied through the matching range, assuming $Q_k = 80$ and $Q_\mu = 25$. Solid lines: $\varepsilon = 0.1$; dashed lines: $\varepsilon = 0.02$; other parameters as for Figure 2.

Suppose that "pure A0 motion" involves bowing-plane bridge displacement αa at the G-string notch, and "pure B0 motion" correspondingly involves bridge displacement βb. Now the generalised forces associated with the applied force are $\alpha F\,e^{i\omega t}$ and $\beta F\,e^{i\omega t}$ respectively. Thus Lagrange's equations for the system are:

$$\ddot{a} + \mu(a + \varepsilon b) = \alpha F\,e^{i\omega t},$$
$$\ddot{b} + kb + \mu\varepsilon(a + \varepsilon b) = \beta F\,e^{i\omega t}, \tag{14}$$

so that for harmonic response,

$$\begin{bmatrix} \mu - \omega^2 & \mu\varepsilon \\ \mu\varepsilon & k + \varepsilon^2\mu - \omega^2 \end{bmatrix} \begin{bmatrix} a \\ b \end{bmatrix} = \begin{bmatrix} \alpha F \\ \beta F \end{bmatrix}. \tag{15}$$

The parameters α and β introduced above suggest a sign convention for the generalised coordinates a and b. One possibility is to define the signs by requiring that α and β are both positive. This works well to define the sign of a, but unfortunately it is not a very satisfactory convention for b since B0-motion involves very little transverse bridge motion, so that β is very small and its sign is not clear. It is better to define the sign of b so as to make ε positive, and we will assume this convention.

A number of transfer functions can now be written down in terms of $a(\omega)$ and $b(\omega)$, the solutions of (15). First, the driving-point admittance at the bridge is

$$Y = i\omega\frac{\alpha a + \beta b}{F}. \tag{16}$$

This is the quantity which determines any influence of the body resonances on the motion of the bowed string, at least within the simplest models of the bowing process [10]. Next, we may define a transfer function to "feel":

$$H_f = \frac{b}{F}. \tag{17}$$

This quantifies the vibration level in the neck of the instrument, which may be felt by the player's left hand. Such

vibration is one possible ingredient of why "matching" is perceived by players as desirable. Next, a useful quantity for comparison with measurements is the transfer function H_p to pressure variation within the box. This pressure will be proportional to the volume fluctuation, so that

$$H_f \propto \frac{a + \varepsilon b}{F}. \tag{18}$$

The constant of proportionality is not needed for the purposes of the experimental comparison.

Finally, it is desirable to estimate the transfer function to far-field radiated sound. We cannot do this with great accuracy without modelling the (complicated) radiation properties of the violin body. At the resonance frequencies of the modes in question here, the wavelength of sound in air is just about long enough for the violin body to be treated as a compact radiator. (This assumption begins to break down for frequencies perhaps an octave higher.) We can thus obtain a useful indication of the radiation by a simple argument. We will suppose that the radiation is the same as that produced by a sphere which has a size comparable with the violin – with a radius of 10 cm, say – and which undergoes the same volume fluctuation as is given by our model. The transfer function to far-field radiated pressure at a distance R is then [11]

$$H_r = \left(\frac{i\omega r/c}{1 + i\omega r/c}\right)\frac{i\omega\rho_0 c\lambda(a + \varepsilon b)}{4\pi r R F}, \tag{19}$$

where r is the radius of the sphere, c is the speed of sound in air and ρ_0 is the ambient air pressure.

All the transfer functions so far defined, being based on equation (15), do not incorporate the effect of damping. They must thus be modified to take account of the damping factors calculated in the previous subsection. This can be done by the usual approach to small modal damping: the poles of each transfer function are shifted off the real axis by the appropriate amounts, but keeping the (real) value of their residues unchanged. We illustrate for the case of the bridge admittance Y. The inverse of the matrix appearing in (15) can be written

$$\frac{1}{(\omega^2 - \omega_1^2)(\omega^2 - \omega_2^2)}\begin{bmatrix} k + \mu\varepsilon^2 - \omega^2 & -\mu\varepsilon \\ -\mu\varepsilon & \mu - \omega^2 \end{bmatrix}, \tag{20}$$

so that

$$Y = i\omega\frac{\alpha^2(k + \mu\varepsilon^2 - \omega^2) + \beta^2(\mu - \omega^2) - 2\alpha\beta\mu\varepsilon}{(\omega^2 - \omega_1^2)(\omega^2 - \omega_2^2)}$$
$$= i\omega\left[\frac{y_1}{(\omega^2 - \omega_1^2)} + \frac{y_2}{(\omega^2 - \omega_2^2)}\right], \tag{21}$$

where

$$y_1 = \frac{\alpha^2(k + \mu\varepsilon^2 - \omega_1^2) + \beta^2(\mu - \omega_1^2) - 2\alpha\beta\mu\varepsilon}{(\omega_1^2 - \omega_2^2)} \tag{22}$$

and

$$y_2 = \frac{\alpha^2(k + \mu\varepsilon^2 - \omega_2^2) + \beta^2(\mu - \omega_2^2) - 2\alpha\beta\mu\varepsilon}{(\omega_2^2 - \omega_1^2)}. \tag{23}$$

Now the damped version of the admittance is given by modifying the denominators of the terms of (21):

$$Y \approx i\omega \left[\frac{y_1}{\omega^2 - \frac{i\omega\omega_1}{Q_1} - \omega_1^2} + \frac{y_2}{\omega^2 - \frac{i\omega\omega_2}{Q_2} - \omega_2^2} \right] . \quad (24)$$

with y_1 and y_2 as above. The same procedure may be followed for the other transfer functions defined in (17)–(19).

3. Results and experimental comparisons

The behaviour of the admittance Y calculated above is shown in Figure 4. Figure 4(a) shows a series of plots of $|Y|$ (on a dB scale) as k/μ varies in 15 equal steps from 0.85 to 1.15. The curves are separated vertically in steps of 5 dB, for clarity. The parameter ε has the (rather large) value 0.05. The curve-veering behaviour is seen clearly, the two peaks never coming very close together. It has been assumed here that $\beta = 0$, which seems a reasonable approximation: the predominant B0 motion is symmetric about the mid-plane of the violin, and will have very little transverse motion at the bridge. Nevertheless, both peaks contribute strongly to the admittance in all cases because of the bridge motion induced by the coupling to A0. Figure 4(b) shows the corresponding set of curves for $\varepsilon = 0.02$, all other values being the same as in Figure 4(a). For most cases, one peak contributes much more strongly than the other, except very close to the matched condition (central curve). The two peaks now approach quite closely. When ε is reduced to 0.01 or below, there is high modal overlap at the matched condition and the peaks merge into one.

We can now make comparisons of the predictions of the model with measurements on a real violin, for validation and to estimate values for the parameters. The test instrument was made by the author, and of middling quality. The strings (Dominant) were tuned to pitch but well damped by means of soft foam near the nut end of the fingerboard. The instrument was suspended from a rigid frame by rubber bands to the four corners, as was done for example by Marshall [3]. The fingerboard had been deliberately adjusted so that in its normal condition, the "predominantly B0" mode was a little higher in frequency than the "predominantly A0" mode. This allows the instrument to be taken through the "matched" condition and beyond, by the simple means of adding mass to the end of the fingerboard. A series of measurements were made, adding successive 1 g masses (of Blutack) to the underside of the free end of the fingerboard. (It may seem counterintuitive to adjust the "effective stiffness" k by adding mass, but this is a consequence of the definition of the generalised coordinates incorporating mass normalisation.) Earlier measurements, made during the process of fingerboard adjustment, had given approximate values of the Q-factors of B0 and A0 when they were well separated in frequency. These values, $Q_k = 80$, $Q_\mu = 25$, will be used in the study of matching effects.

The clearest results for the purpose of comparison with the theoretical model come from measuring the transfer function
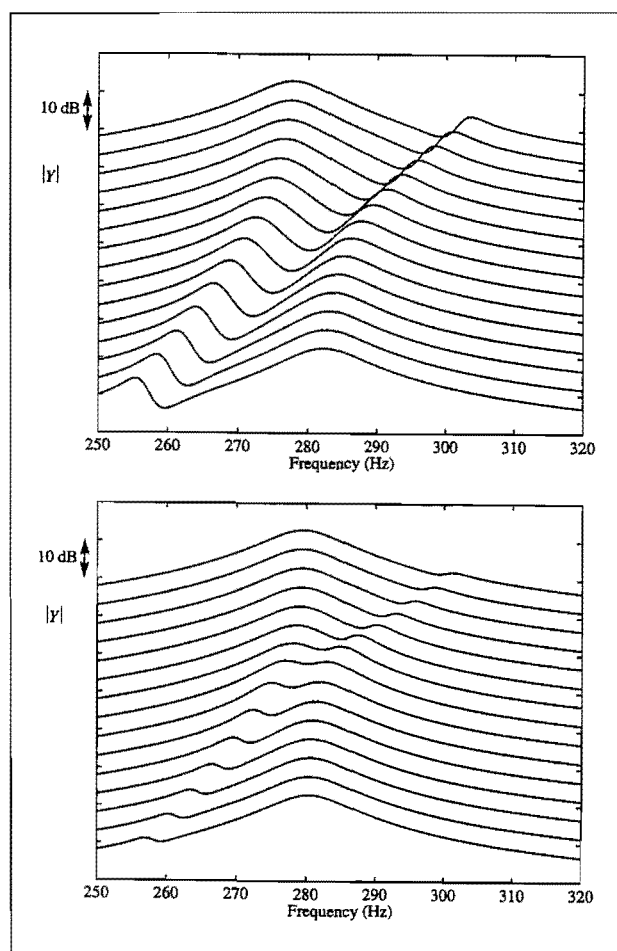

Figure 4. Variation of driving-point admittance at the bridge, Y, for (a) $\varepsilon = 0.05$ and (b) $\varepsilon = 0.02$. Top curves: $k/\mu = 1.15$; bottom curves: $k/\mu = 0.85$; intermediate curves showing 14 equal increments between these limits. Curves are separated by 5 dB steps for clarity.

H_p from excitation at the bridge to the internal sound pressure within the box. The G-string corner of the bridge was tapped with a soft-tipped hammer, in the direction of the bowing plane, and the response measured by a small electret microphone inserted through the treble f-hole to lie close to the bottom block. The result was captured by a PC-based data-logger sampling at 5 kHz, and the transfer function calculated by FFT in the normal way. Results are shown in Figure 5(a). The four plots, again spaced by 5 dB for clarity, show the violin in its normal state in the top curve, then after loading with 1 g, 2 g and 3 g masses.

These results are to be compared with Figure 5(b), which shows the corresponding theoretical plot with parameter values approximately matched to the measurement. (Since the range of theoretical plots is not limited by the baseline state of the actual violin, one more curve is plotted here so that the set shown is exactly symmetric about the "matched" condition.) The real violin has additional modes, of course, producing some fine detail at the lower frequencies, but good agreement over the central frequency range is evident. The pattern of frequency variation is well reproduced. The variation of
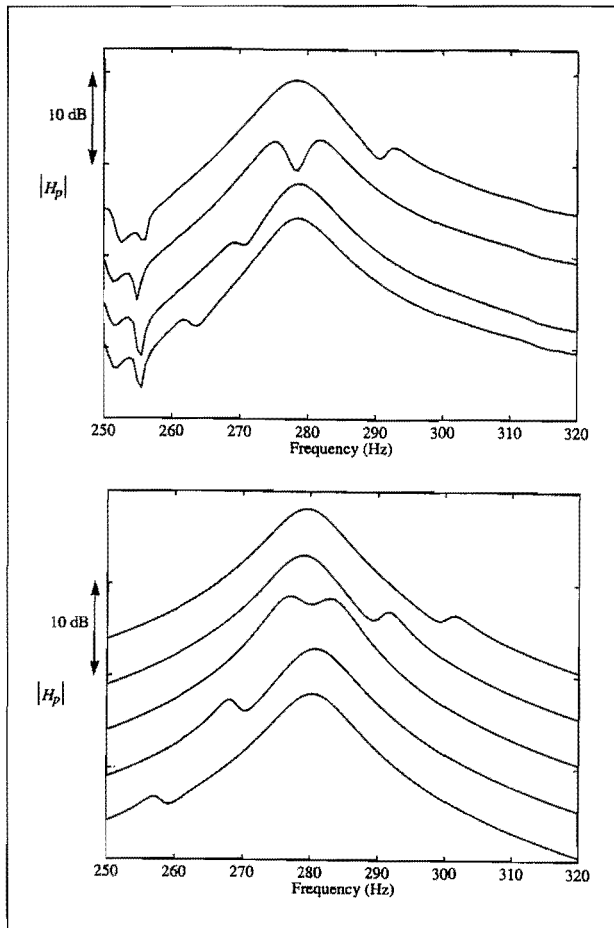
Figure 5. Transfer functions H_p from driving at the bridge to internal pressure in the box (a) as measured on a freely-suspended violin; (b) as predicted by the theoretical model with $\varepsilon = 0.02$. For the measurements, successive 1 g masses were added to the end of the fingerboard, the original state of the violin being shown in the top curve. For the theoretical comparison, k/μ is varied in five equal steps from 1.15 (top) to 0.85 (bottom). Curves are separated by 5 dB steps for clarity.

Figure 6. Transfer functions to "feel", H_f, (a) as measured on a freely-suspended violin; (b) as predicted by the theoretical model . Details are as in Figure 5 except that the curves are not separated in this case.

damping factors is not matched perfectly, but the agreement is acceptable. It is clear that the violin is "matched" when loaded with 1 g. The addition of each 1 g mass to the end of the fingerboard produces a shift in frequency of the "predominantly B0" mode of about 8 Hz, and corresponds to a change in k/μ of approximately 7%. From the separation of the two peak frequencies in the second curve of Figure 5(a), and using equation (6), it may be deduced that $\varepsilon \approx 0.02$. This is the value used to compute Figure 5(b).

Now that we have values for all the model parameters, we can predict a different transfer function and compare it to corresponding measurements. An interesting quantity to examine is the transfer function to "feel", H_f, defined in equation (17). To obtain a measurement comparable with this, the violin was tapped with the soft hammer on the back of the scroll, and the response was measured using a small accelerometer (weighing less than 1 g) glued to the G-string corner of the bridge and acting in the direction of the bowing plane. By the principle of reciprocity this is proportional to
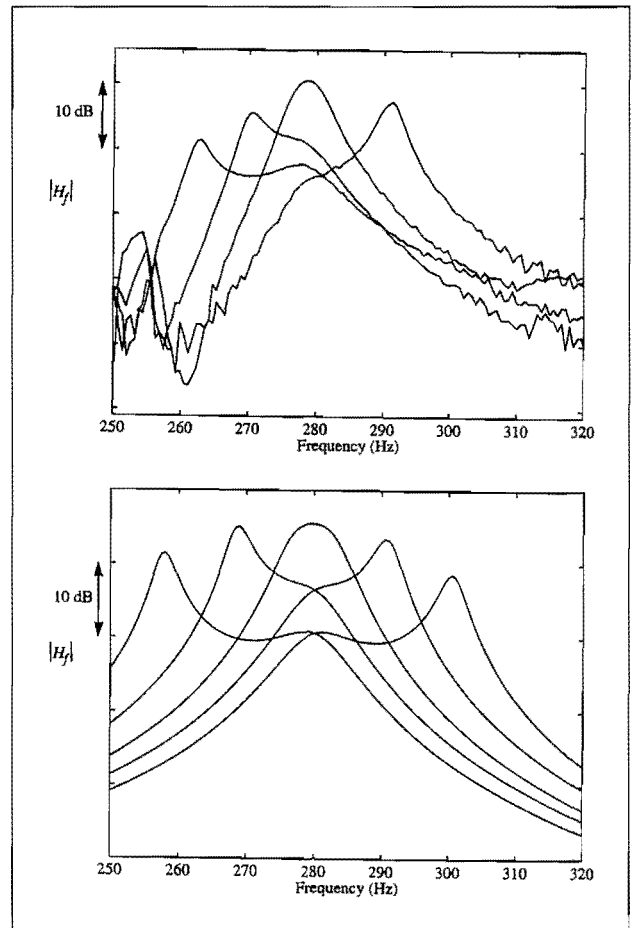
the transfer function as defined earlier. The comparison of measurement and theory is shown in Figure 6. The format is the same as Figure 5, except that here the curves are more clearly visible when not separated in a "waterfall" display. The agreement is very satisfactory, and gives some confidence in the theoretical model developed in the previous section.

Finally, we examine the effect of "matching" on the far-field sound radiation, through the transfer function H_r defined in (19). It was not possible to make corresponding measurements in this case. Also, the value of the parameter λ was not known, without which it is not possible to predict absolute levels. Figure 7 shows the predicted behaviour, for the same range of parameter values as Figures 5(b) and 6(b). The curves are not separated here – although this makes it a little hard to follow the individual lines, it shows immediately the important fact that by the extremes of the frequency range plotted, all the curves reach essentially the same levels. The effect on radiated sound of "matching" is confined to frequencies close to the two modes in question. There is no long-range effect. We return to this observation later.

It appears from Figure 7 that near the matched condition the radiation levels are rather higher near the two resonant
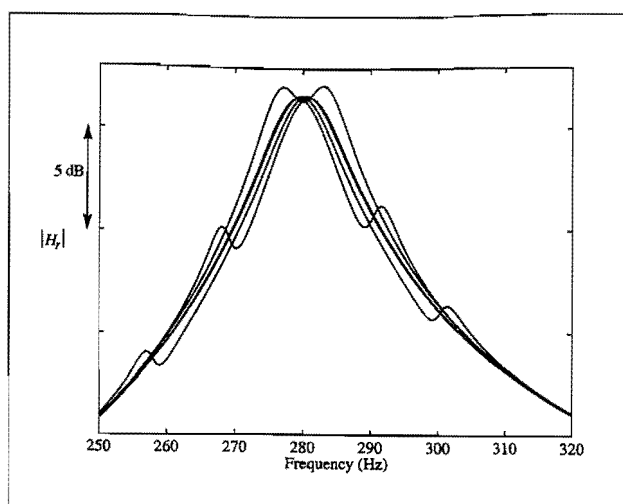
Figure 7. Approximate transfer functions to far-field radiated sound, H_r, as predicted by the theoretical model . Details are as in Figure 5(b) except that the curves are not separated in this case.
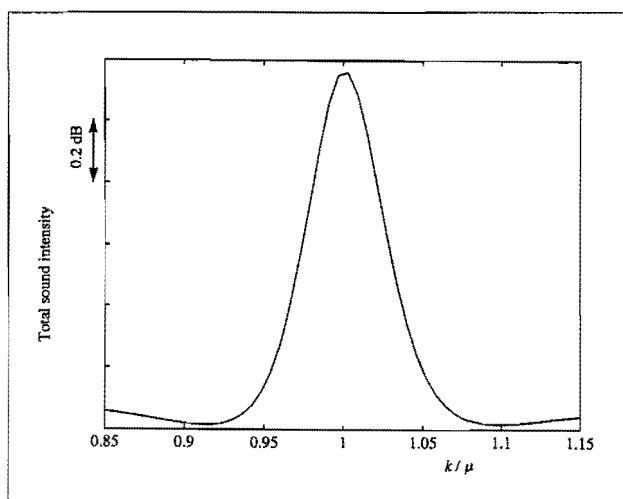

Figure 8. Variation of "total sound intensity" as k/μ is varied through the matching range, showing a small enhancement close to the matched condition.

peaks. To quantify this, it is useful to compute a measure of the total radiated sound intensity as a function of k/μ. The integrated value of $|H_r|^2$ over all frequencies gives such a measure. Figure 8 shows this quantity for the parameter values used here. There is indeed an increase in total sound radiation very close to the "matched" condition, by about 1.1 dB here. Further studies reveal that this depends critically on the value of the coupling parameter ε. When this is small enough that there is significant modal overlap in the matched state, then the value rises to 3 dB. When ε is bigger so that the peaks are well separated, as in Figure 4(a), the total sound radiation is essentially unchanged throughout the matching process. The value used here, $\varepsilon \approx 0.02$, is on the boundary between these two extreme cases.

4. Discussion

4.1. Implications for the matching procedure

The model developed here sheds light on the sound and playing properties of matched and unmatched violins, but before discussing that issue in detail there is an important consequence for the violin maker who wishes to achieve matching. Some makers rely entirely on their ears for detecting the frequencies of the two modes which are being adjusted. When the modes are well separated it is usually quite easy to hear A0 by blowing gently across an f-hole, and to hear B0 by holding the instrument body at a nodal point, and tapping and listening on the scroll or on the end of the fingerboard. However, it will be apparent from the account of "veering" behaviour given above that close to the matched condition, it may be rather hard to distinguish separately the two modes by this method, since the two types of motion are coupled together. Unreliable results are likely.

Many makers try to get round this problem by using simple measurement technology to detect the two frequencies. Typically, the instrument might be supported on soft foam blocks above a loudspeaker which is driven by a sine-wave oscillator. Resonant frequencies might be detected by a microphone inside the body cavity, or by the Chladni-pattern approach of watching for bounce of a powder. (A common technique is to fix a small "cup" made from the packaging of pills to the fingerboard end, and put a little powder in the cup [12].) Such methods are certainly more reliable than relying on the ear, but there is still a pitfall associated with the method of driving the violin, which might give misleading results near the matched condition.

In the method described, the loudspeaker drives body vibration by applying a distributed force to the back of the instrument. The response to such driving can be analysed by the same method as was used in section 2.2 – all that is needed is new values for the parameters α and β, to represent the generalised forces arising from this loudspeaker drive. Presumably both of these parameters will have non-negligible values, in contrast to driving at the bridge where a reasonable approximation was to take $\beta = 0$. Now recall the discussion of the changes to mode shapes during the "veering" process illustrated in Figure 2. If the new values of α and β have the *same sign*, then at some stage along the curve followed by the lower of the two frequencies the two contributions will cancel exactly. This means simply that the mode shape will have a nodal line passing symmetrically over the loudspeaker, so that it cannot be excited by a loudspeaker in that position. The higher of the frequencies will not exhibit this cancellation. Conversely, if α and β have *opposite signs*, then the cancellation will occur at some point for the higher frequency, the lower frequency being unaffected.

The upshot of this, for the maker, will be that at a particular stage in the matching process one of the two modes will "disappear". Only a single peak will be seen, and it would be easy to be misled into supposing that matching had then been achieved. But this need not be the case at all. The disappearance of one mode is due entirely to the position of
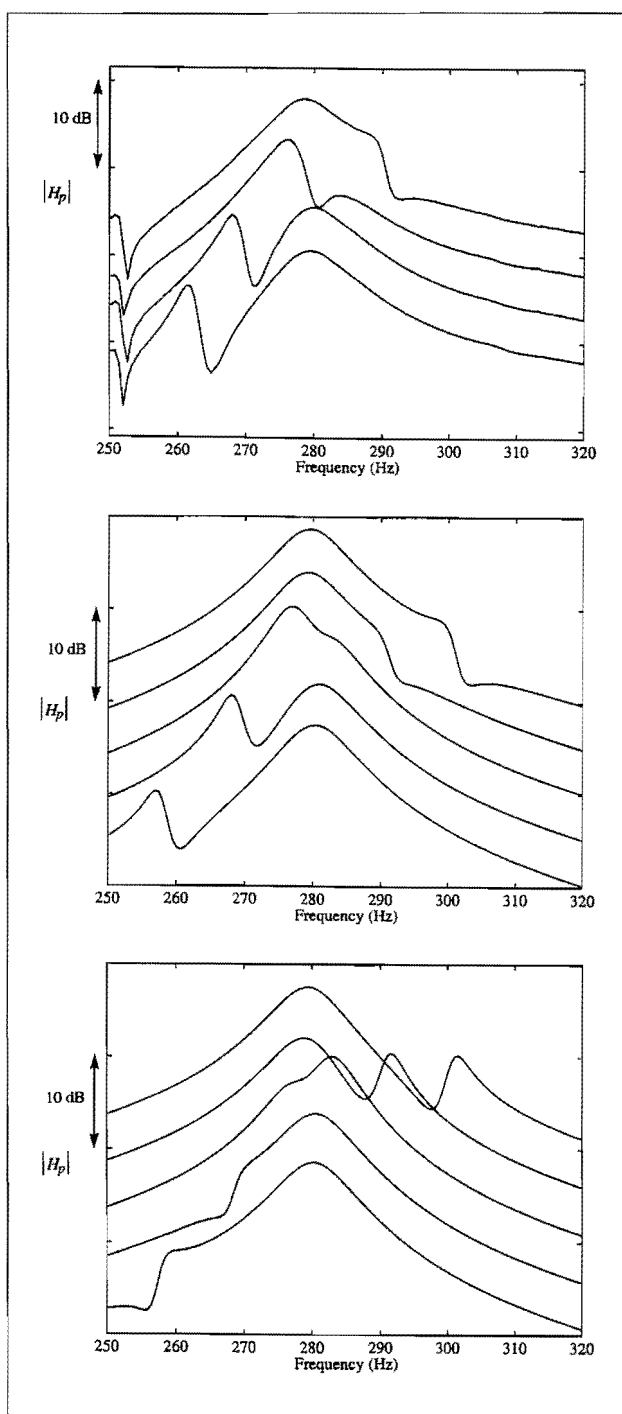
Figure 9. Transfer functions from driving at the centre of the back to internal pressure inside the box (a) as measured on a freely-suspended violin; (b) as predicted by the theoretical model with $\alpha = 1$, $\beta = -0.5$; (c) as predicted by the theoretical model with $\alpha = 1$, $\beta = 0.5$. Details are as in Figure 5.

the loudspeaker, not to the relative frequencies of the modes. Driving the body in a different way would restore the missing mode to view.

This behaviour can be illustrated, both using the theoretical model and by making a further set of measurements on the test violin. Loudspeaker driving is not convenient for these measurements, but much the same effect can be created

by hitting with the soft hammer in the centre of the back of the instrument. By measuring with the internal microphone as before, we simulate one of the violin maker's methods described above. A set of results in the same format as Figure 5(a) is shown in Figure 9(a). As before, the matched case corresponds to the second curve from the top, with 1 g added to the fingerboard. This curve shows two peaks, but the top curve exhibits the cancellation behaviour just described, and only shows a single peak. A maker might conclude erroneously that matching was achieved in this latter case.

The fact that the higher of the two frequencies shows cancellation immediately tells us that α and β must have opposite signs for driving at this particular place (and using the sign convention introduced earlier, so that ε is positive). A reasonable match to this figure is obtained from the theoretical model by using values $\alpha = 1$, $\beta = -0.5$, as is shown in Figure 9(b). The corresponding case with $\alpha = 1$, $\beta = 0.5$ is shown in Figure 9(c). As expected, cancellation now occurs with the lower mode and the pattern is quite different from that shown by the measurement.

4.2. Implications for the behaviour of instruments

Now at last we can turn to the question of why a matched instrument might be perceived as better or worse than an unmatched one. The most immediate deduction from all the transfer functions shown earlier is that the effect of varying the stiffness ratio k/μ is confined to frequencies close to the two modes in question. There is no effect on admittance, "feel" or radiated sound at more remote frequencies, although all three of those quantities show characteristic variations within the narrow frequency range covered by the two resonances. The relevance of this remark to violin playing needs careful examination.

A bowed string applies force to the bridge over a wide range of frequencies. This frequency spectrum can be divided into two components. A long, steady note generates strong signal at harmonics of the fundamental frequency. With vibrato, the energy is spread into bands around each harmonic. If this were the only input from the string to the body, it is hard to believe that the effects of "matching" would be described in such glowing terms by players. All effects would be confined entirely to the fundamentals of notes around C, C# and D in first position on the G and D strings. Any playing test in which those three notes were avoided should be *incapable* of showing any distinction between a matched and an unmatched instrument.

No systematic psychoacoustical experiment to test this idea has been attempted, but it seems clear from less formal evidence that an experienced player is perfectly capable of performing this apparently impossible feat of discrimination. This suggests that the second component of the frequency spectrum of string force is crucial. Violin playing does not, of course, consist entirely of long, steady, legato notes. Different bowing gestures are used to generate notes with a wide variety of starting and finishing transients, and in general terms the details of such transients are known to be crucial to the perception of "tone quality" (see for example

Risset and Wessel [13]). In terms of frequency components, transients generate broad-band signals which have the potential to excite *all* the resonances of an instrument to a greater or lesser extent. Some bowings, such as the martelé, generate particularly strong broad-band signal, others much less. It has been suggested that the sound generated by transients such as martelé notes might be particularly effective at conveying information about body resonances, because of a peculiarity of human hearing known as the "precedence effect" [14].

Once the body resonances have been excited to some degree, there is scope for a variety of effects occurring. The sound could be influenced directly, through radiation. The "feel" could be affected, because neck vibration may be felt by the player's left hand. Finally, and least obviously, the motion of the string itself could be influenced by feedback from the bridge motion which might influence the bow-string interaction in subtle ways. Are any of these things actually influenced significantly by "matching"? The obvious mechanism for such an influence is that close to the matching condition the A0 and B0 motions are coupled and mixed, as has been explained earlier.

It does not seem likely that there is a strong influence of matching on the bowing process: the changes in admittance shown in Figure 4(b) are rather slight, and such experience as is available with the bowed-string problem does not suggest great sensitivity to such changes. The story is different for "sound" and "feel", though. For an instrument which is far from the matched state, we have argued that B0 will not be driven at all efficiently by the string. Achieving sufficiently close matching that the instrument is within the range of "veering" behaviour will mean that both modes can be driven by the string (because they involve some A0 motion), both can radiate sound (because they involve some volume change), and both will contribute to "feel" (because they involve some B0 motion). Informal tests with an experienced player so far seem to suggest that the main cues by which a player is able to judge whether an instrument is close to the matched state come from "feel" more than from sound.

All these factors are potentially desirable from the player's point of view, and suggest a rationale for preferring instruments to be matched, at least closely enough to enter the "veering" range. Just how close that needs to be in practice depends on the value of the coupling parameter ε. Informal evidence from makers suggests that this value might vary quite a bit among different instruments. It is far from clear what features of the instrument construction influence ε. Recall that this parameter quantifies the amount of volume change associated with B0-motion. As far as the "box" is concerned, B0 involves motion in response to an oscillating moment applied at the top block, in reaction to the vibration of neck and fingerboard. Volume change might perhaps arise from differential distortion of the top and back plates in response to this moment. Perhaps the general arching form, or the depth and configuration of purfling channel, have an influence? In principle, the volume change could be deduced directly from a sufficiently detailed experimental modal analysis. All this would make an interesting topic for further research
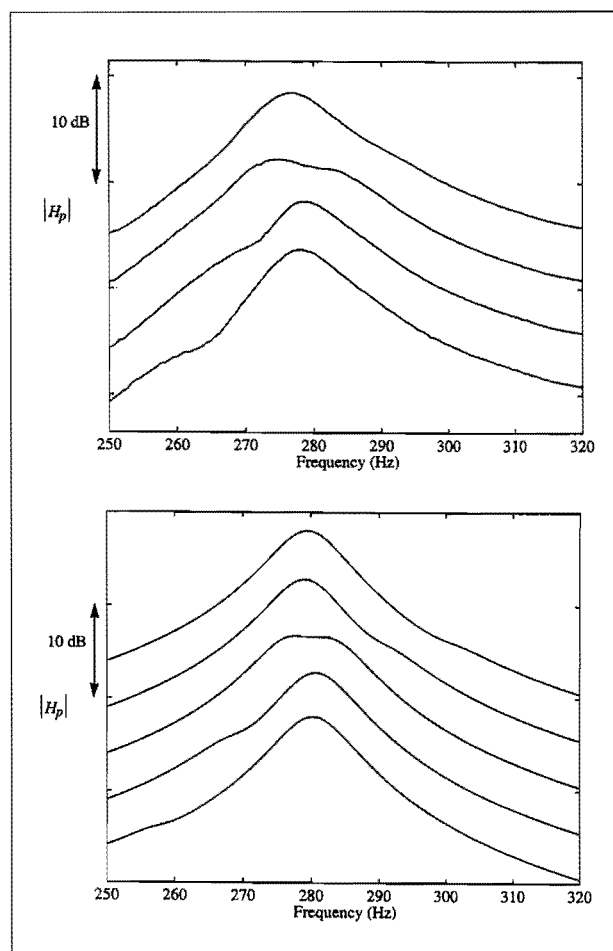

Figure 10. Transfer functions H_p from driving at the bridge to internal pressure in the box (a) as measured on a violin held by a player; (b) as predicted by the theoretical model with parameter values as in Figure 5(b) except that $Q_k = 30$.

The hypotheses put forward here could be probed by fairly straightforward playing tests. An instrument can be put into and out of the matched state easily, using added mass as was done in the experiments reported in the previous section and as has been done by Hutchins [4] and others. A player could be offered a violin repeatedly, not knowing which times it had the added mass or did not have it. Their task would be to decide which state it was in. In different tests they would be asked to try to make this judgement based on limited information: playing only on one particular string; playing only slow legato scales; playing martelé, or spiccato, or sautillé and so on. Perhaps they might even be asked to play with a fingerless glove on the left hand, to cut down information about "feel". The predictions would be: "feel" might be a more sensitive indicator than sound; the G string or D string should be much easier to judge than the A string or E string; vigorous bowings like martelé should prove more discriminating than legato. It would intriguing to find out whether a good player can tell the difference at all when restricted to legato bowing and a test passage which avoided the critical notes of C, C# and D.

There is one final step in the physical investigation of this problem. All the measurements and theoretical comparisons have related to a "free" instrument, suspended on rubber bands. It is reasonable to enquire what happens to the coupled modes we have investigated when the instrument is held by a player in the conventional way. It seems possible that carefully-achieved matching might be upset by added mass or stiffness effects from the player's body. The measurement shown in Figure 5(a) was repeated while the violin was held using a normal shoulder rest (Resonans) and chin rest, with the left hand holding the neck conventionally in first position. The result is shown in Figure 10(a). What is revealed here is that, as one might have anticipated, the damping has increased substantially, especially the damping of B0 which was previously rather low. The frequencies, though, do not seem to have been affected significantly by effects of holding. The second curve from the top shows the two peaks having comparable heights, indicating that this is still close to the matched state. Figure 10(b) shows the result of the theoretical model as in Figure 5(b), but with Q_k decreased from 80 to 30. This produces reasonable agreement with Figure 10(a), showing that this single parameter change really does capture most of the difference between the two cases.

5. Conclusions

A simple two-degree-of-freedom model has been developed, which allows the process of "A0-B0 matching" in the violin to be simulated. A variety of relevant transfer functions can be calculated. The model has been compared with measurements on a violin and good agreement has been demonstrated, both in details of transfer functions and in the general "curve-veering" behaviour shown by the mode frequencies. The comparison allows values of all the model parameters to be estimated for this particular violin. It would be of some interest to find out whether these values, especially that of the coupling parameter ε, vary significantly among different violins.

The effect of "matching" has been shown to be confined to frequencies close to the two modes in question. This means that any audible or tactile consequences based entirely on the playing of long steady notes would be confined to just a few notes in first position on the G and D strings. The fact that many players report a more wide-ranging influence suggests an important role for the broad-band input applied to the

violin body by the string associated with bowing transients. The model suggests some definite predictions for the conditions under which a player might and might not be able to distinguish a matched from an unmatched instrument in a blind test. These have yet to be systematically tested.

Acknowledgement

References

[1] L. Cremer: The physics of the violin. MIT Press, Cambridge, Mass., 1985.

[2] J. A. Moral, E. V. Jansson: Eigenmodes, input admittance, and the function of the violin. Acustica 50 (1982) 329–337.

[3] K. D. Marshall: Modal analysis of a violin. J. Acoust. Soc. Amer. 77 (1985) 695–709.

[4] C. M. Hutchins: Effects of an air-body coupling on the tone and playing qualities of violins. J. Catgut Acoust. Soc. 44 (1985) 12–15.

[5] J. C. Schelleng: The violin as a circuit. J. Acoust. Soc. Amer. 35 (1963) 326–338.

[6] E. A. G. Shaw: Cavity resonance in the violin: network representation and the effect of damped and undamped rib holes. J. Acoust. Soc. Amer. 87 (1990) 398–410.

[7] C. H. Hodges, J. Woodhouse: Theories of noise and vibration transmission in complex structures. Rep. Prog. Phys. 49 (1986) 107–170. See §2.2.

[8] N. C. Perkins, C. D. Mote: Comments on curve veering in eigenvalue problems. J. Sound Vib. 106 (1986) 451–463.

[9] M. E. McIntyre, J. Woodhouse: The influence of geometry on linear damping. Acustica 39 (1978) 209–224.

[10] J. Woodhouse: On the playability of violins, part i: reflection functions. Acustica 78 (1993) 125–136.

[11] A. P. Dowling, J. E. Ffowcs Williams: Sound and sources of sound. Ellis Horwood, Chichester, 1983, See §2.3.

[12] A. Ekwall: Blister cup indicators and bm-values as aids when indicating body resonances B1, B0 and B−1. J. Catgut Acoust. Soc. 2 8 (1995) 14–16.

[13] J. C. Risset, D. L. Wessel: Exploration of timbre by analysis and synthesis. – In: The psychology of music. D. Deutch (ed.). Academic Press, New York, 1982.

[14] J. Woodhouse: On recognising violins: starting transients and the precedence effect. Catgut Acoust. Soc. Newsletter 39 (1983) 22–24.